WEB TENSION BEHAVIOR IN THE PRESENCE OF ECCENTRIC ROLLERS: MODELING AND VALIDATION

By

C. Branca, P. R. Pagilla, and K. N. Reid
Oklahoma State University
USA

ABSTRACT

Since rotating machinery is used to transport the web on rollers, it is common to observe periodic oscillations in measured signals such as web tension and web transport speed. These periodic oscillations are more prevalent in the presence of non-ideal machine elements such as eccentric rollers and out-of-round material rolls. One of the main objectives in transport of webs is to maintain tension at a prescribed value. Tension regulation affects almost all key aspects of web transport including printing, registration, wrinkle formation, winding, etc. Therefore, models of web tension and web transport velocity in the presence of non-ideal rollers which can accurately predict measured behavior will be beneficial to the analysis of web transport under various dynamic conditions and in the design of suitable control systems.

The focus of this paper is on modeling the effect of eccentric rollers on web tension. The governing equations for web velocity on an eccentric roller and web tension in spans adjacent to the eccentric roller are presented and discussed. To solve these governing equations, one requires the knowledge of the entry and exit point of the web on the eccentric roller as it rotates and the length of web spans adjacent to the eccentric roller; a method in obtaining this information is described. To corroborate the models and the developed approach, data from experiments on a web platform are compared with model simulations and results are presented and discussed.

NOMENCLATURE

A	Area of cross section of the web [ft^2]
ABC	Triangle having the points A, B, and C as vertices
$\overline{AB}$	Line segment with ending points A and B
$A\hat{B}C$	Angle between line segments $\overline{AB}$ and $\overline{BC}$
C_G	Geometric center of the roller
C_R	Center of rotation of the eccentric roller
b	Idle roller viscous friction coefficient $\left[\frac{\text{lbf ft}}{\text{rad/s}}\right]$
c	Idle roller constant friction torque [lbf ft]
d	Distance between geometrical centers of rollers [ft]
d_0	Distance between centers of rotation of rollers [ft]
d_{en}	Distance between the center of rotation and the web entry point on the roller [ft]
d_{ex}	Distance between the center of rotation and the web exit point on the roller [ft]
E	Modulus of elasticity (Young's modulus) $\left[\frac{\text{lbf}}{\text{ft}^2}\right]$
e	Roller eccentricity (distance between the center of rotation and geometric center) [ft]
f_0	Fundamental frequency of the disturbance induced by the eccentric roller [Hz]
g	Gravitational acceleration
L	Free span web length [ft]
P	Web entry point on an eccentric roller
q	Web exit point on an eccentric roller
R	Radius of the roller [ft]
T_i	Web tension in the i-th span [lbf]
v	Web velocity (or peripheral velocity of the roller) [FPM]
ω	Roller angular velocity [rad/sec]
θ	Roller angular displacement [rad]
τ_f	Idle roller friction torque [lbf ft]

INTRODUCTION

Modeling of longitudinal behavior of the web as it is transported on rollers has been addressed in several papers, examples include [1–3]. Most of the existing standard models in literature assume ideal behavior of all the machine components in the web line. As a consequence these models do not reproduce the tension oscillations that are commonly seen in practical web lines. Since rollers and rotating machinery are primarily involved in transport of webs, the measured web tension signal often contains oscillations of periodic nature. These periodic oscillations (disturbances) in the web tension signal are typically generated by non-ideal machine components, effects and resonances. Some non-ideal effects that deteriorate web tension regulation performance include the presence of eccentric or out-of-round idle rollers and material rolls, backlash in mechanical transmission systems, and compliance in machine components or shafts transmitting power. Our prior work in [4] initiated a discussion on model validation

and identification of source of oscillations in tension signals. The effort was focused on analyzing the existing web span tension model and making necessary refinements to the models to better correlate the data obtained from model simulations and experiments. One key aspect that was identified is that the change in span length that is adjacent to an eccentric or out-of-round roller causes tension oscillations. The web span tension model was refined to include the change in span length due to non-ideal rollers. This led to a better prediction of experimentally observed tension behavior by the model, and required computation of changing span length for spans that are adjacent to the non-ideal rollers. Numerical algorithms for computing span length adjacent to non-ideal rollers were reported in [5]. The focus in this paper is to further develop the models to reflect experimentally observed behavior. In particular, this paper will consider the development of a governing equation for web velocity on an eccentric roller. In addition, an analytical expression for computation of span length that is adjacent to an eccentric roller will also be derived. The paper will also discuss the relevant model simulations and experiments conducted to highlight the improvements made by these new results to the developments reported in [4, 5].

From the analysis of the frequency content of the measured tension signal, oscillations due to an eccentric roller can be distinguished. In particular, given the line speed and the radius of the eccentric roller, one can identify the fundamental frequency of the oscillations and its higher order harmonics. In order to reproduce in model simulations both the fundamental frequency and its harmonics, it is necessary to modify the governing equations for web velocity on the non-ideal roller and web span tension. Specifically, because of the eccentricity of the roller, the governing equation for the eccentric roller angular velocity must be modified to include the additional torque acting on the roller due to the fact that the center of mass and the center of rotation are not coincident. Moreover, the torques on the eccentric roller due to the tensions in web spans adjacent to the eccentric roller will be different and are functions of the angular position of the roller because the wrap angle changes with the rotation of the eccentric roller. These aspects will be discussed in the paper, and a governing equation for web velocity on an eccentric roller will be developed. Further, derivation of a closed form expression for the web span length as function of the angular displacement of the eccentric roller will be given. By including the closed form expression for the web span length in the span tension model, one can improve the accuracy of the model simulations. In addition, the closed form expression facilitates better understanding of the intrinsic connection between the dynamics of the rotational motion of the eccentric roller and the tension behavior in the spans, which provides insights into why higher order harmonics are found in the tension signal. To verify that these new models provide improved correlation between model simulations and experiments, experiments were performed on a large web platform. Comparison of the data from experiments and model computer simulations show that the new models are able to closely predict experimentally observed behavior.

MODELS FOR WEB VELOCITY AND TENSION IN THE PRESENCE OF AN ECCENTRIC ROLLER

The following modified governing equation for web tension which includes the effect of the span length changes was presented in [4]:

$$\dot{T}_i(t) = \frac{v_i(t)(EA - T_i(t)) - v_{i-1}(t)(EA - T_{i-1}(t))}{L(t)} + \frac{(EA - T_i(t))\dot{L}(t)}{L(t)}. \qquad \{1\}$$

The solution of the above governing equation requires computation of the span length. Numerical algorithms to compute the span length in the presence of an eccentric roller and an elliptically shaped material roll were presented in [5]. In this paper some of the results in [5] will be extended and a closed form expression for the span length adjacent to an eccentric roller will be derived. The span length and its derivative will be computed as function of the angular displacement and the velocity of the eccentric roller. To reproduce all the harmonics in the measured tension signal due to the presence of the eccentric roller it is not sufficient to include only the effect of the span length but it is also necessary to modify the governing equation for web velocity on the eccentric roller which will be the focus in this section.

A roller is said to be eccentric if the center of rotation and the geometric center do not coincide, and the deviation from the geometric center to the center of rotation is called the eccentricity of the roller. The motion of an eccentric roller will affect web tension in adjacent spans via the influence on two aspects: (1) change in length of the spans adjacent to the roller and (2) additional (gravity induced) torque acting on the eccentric roller due to imbalance will result in a different surface velocity at each point on the eccentric roller. These two issues will be discussed in this section. The length of the web in the spans adjacent to the eccentric roller as a function of its angular displacement will be derived first followed by an appropriate modification of the governing equation of the eccentric roller. The derivation of the length of web spans adjacent to the eccentric roller will also serve as a means to introduce various definitions and concepts which are subsequently needed.

Derivation of length of web spans adjacent to an eccentric roller

In this section, a span where the downstream roller is eccentric and the upstream roller is ideal will be considered. For deriving the web span length between the two rollers one has to determine the points where the web leaves the upstream ideal roller and the point where the web enters the downstream eccentric roller. For the eccentric roller the point at which the web leaves that roller changes with the rotation of the roller; therefore, one has to determine this point dynamically as a function of the angle of rotation of the roller.

We will first consider a span between two ideal rollers for the initial setup of the problem, and we will subsequently modify the downstream roller to an eccentric roller. Two configurations are possible for a web span between any two rollers – underwrap and overwrap. These are shown in Fig. 1. The under-wrap configuration shown in Fig. 1(a) is considered first. Since the line segment $\overline{ED}$ is tangent to both the rollers, the two right-angled triangles AEB and ADC are similar. Therefore, the angles $A\widehat{B}E$ and $A\widehat{C}D$ are equal, and so are the angles $B\widehat{A}E$ and $C\widehat{A}D$. This fact will be used to derive an equation for the length of the segment $\overline{DE}$.

(a) Under-wrap Configuration

$R_1 = \overline{BE}$　　　$d = \overline{BC}$　　　$R_2 = \overline{CD}$

(b) Over-wrap Configuration

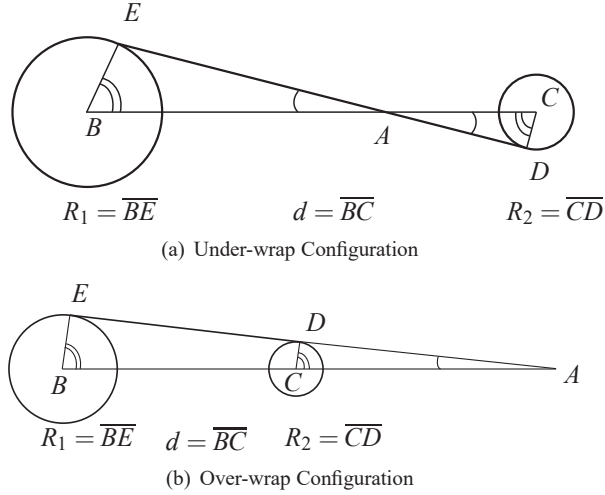$R_1 = \overline{BE}$　$d = \overline{BC}$　$R_2 = \overline{CD}$

Figure 1: Idle Roller Under-Wrap and Over-Wrap Configurations

The angles $A\widehat{B}E$ and $A\widehat{C}D$ being equal results in

$$\frac{R_1}{\overline{AB}} = \frac{R_2}{\overline{AC}} \quad \Rightarrow \quad \overline{AB} = \overline{AC}\frac{R_1}{R_2}. \qquad \{2\}$$

Also, the distance between the center of the rollers is given by

$$d = \overline{AB} + \overline{AC}. \qquad \{3\}$$

Solving {2} and {3} results in

$$\overline{AC}(d) = \frac{d}{1 + \frac{R_1}{R_2}}. \qquad \{4\}$$

Therefore, the angle $A\widehat{C}D$ as function of $\overline{AC}$ is given by

$$A\widehat{C}D(d) = \text{acos}\frac{R_2}{\overline{AC}(d)}. \qquad \{5\}$$

To define the coordinates of the contact points which will be used to determine web span length, one must define an appropriate coordinate axis. To do this it is simpler to first consider a span between two ideal rollers. Consider a coordinate axis located at the center of the upstream roller with its abscissa (called as x-axis) along the line joining the two rollers.

Given the Cartesian coordinates for $B \equiv (X_B, Y_B)$ and $C \equiv (X_C, Y_C)$, the coordinates for $D(d)$ and $E(d)$ are

$$D(d) \equiv (X_D, Y_D) = \begin{bmatrix} X_C - R_2\cos(A\widehat{C}D(d)) \\ Y_C - R_2\sin(A\widehat{C}D(d)) \end{bmatrix},$$

$$E(d) \equiv (X_E, Y_E) = \begin{bmatrix} X_B + R_1\cos(A\widehat{C}D(d)) \\ Y_B + R_1\sin(A\widehat{C}D(d)) \end{bmatrix}, \qquad \{6\}$$
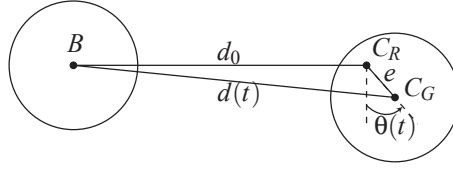
51

Figure 2: Eccentric idle roller: C_G is the geometric center, C_R is the center of rotation, e is the eccentricity, d_0 is the distance between the centers of rotation of the two rollers, and $d(t)$ is the distance between the geometric centers of the two rollers.

and the span length is given by

$$L(d) = \sqrt{(X_D(d) - X_E(d))^2 + (Y_D(d) - Y_E(d))^2}. \qquad \{7\}$$

By substituting the previous expressions in {7} a simplified expression for the span length may be derived, which is given below:

$$L(d) = \sqrt{d^2 - R_1^2 + 2R_1R_2 - R_2^2}. \qquad \{8\}$$

In the presence of an eccentric idle roller the distance d between the geometric centers of the idle rollers varies with the rotation of the eccentric roller because the center of the eccentric idler will be rotating. In order to use the previous procedure it is necessary to determine the value of $d(t)$. Let d_0 be the distance between the centers of rotation and e be the eccentricity (see Fig. 2). The expression for $d(t)$ is given by

$$\begin{aligned} d(t) &= \sqrt{(d_0 + e\sin(\theta(t)))^2 + (e\cos(\theta(t)))^2} \\ &= \sqrt{d_0^2 + 2e\,d_0\sin(\theta(t)) + e^2} \end{aligned} \qquad \{9\}$$

where $\theta(t)$ is obtained by the integration of the governing equation of the eccentric roller. The closed-form equation for the span length in the case of an eccentric roller is obtained by combining {8} and {9}:

$$L(t) = \sqrt{d_0^2 + 2e\,d_0\sin(\theta(t)) + e^2 - R_1^2 + 2R_1R_2 - R_2^2}. \qquad \{10\}$$

The time derivative of span length also appears in the governing equation for web tension in a span (see {1}); this is given by differentiating {10}:

$$\dot{L}(t) = \frac{d_0 e\omega(t)\cos(\theta(t))}{L(t)} \qquad \{11\}$$

where $\omega := \dot{\theta}$ is the angular velocity of the eccentric roller.

A similar approach can be taken to develop the span length for the over-wrap configuration. The first step is to find an expression for the length L as function of the distance between the geometric centers of the rollers (see Fig. 1(b)). In this case the

angles $B\widehat{A}E$ and $C\widehat{A}D$ are equal. Since the triangles AED and ADC are right-angled, it is possible to find the sine of the angle $B\widehat{A}E$:

$$\sin(B\widehat{A}E) = \frac{R_2}{\overline{AC}} = \sin(C\widehat{A}D) = \frac{R_1}{\overline{AB}} = \frac{R_1}{d + \overline{AC}}. \tag{12}$$

Solving the above equation for $\overline{AC}$ gives

$$\overline{AC}(d) = \frac{R_2 d}{R_1 - R_2} = \frac{d}{\frac{R_1}{R_2} - 1}. \tag{13}$$

From $\overline{AC}(d)$ it is possible to find the angle $A\widehat{C}D$ as

$$A\widehat{C}D(d) = \mathrm{acos}\frac{R_2}{\overline{AC}(d)}. \tag{14}$$

The angle $A\widehat{C}D$ is also equal to $B\widehat{A}E$, which can be used to find the coordinates of the points $D(d)$ and $E(d)$:

$$D(d) \equiv (X_D, Y_D) = \begin{bmatrix} X_C + R_2 \cos(A\widehat{C}D(d)) \\ Y_C + R_2 \sin(A\widehat{C}D(d)) \end{bmatrix}$$

$$E(d) \equiv (X_E, Y_E) = \begin{bmatrix} X_B + R_1 \cos(A\widehat{C}D(d)) \\ Y_B + R_1 \sin(A\widehat{C}D(d)) \end{bmatrix} \tag{15}$$

Note that $d(t)$ in the over-wrap case is also given by {3}. Substitution of $d(t)$ obtained using {3} into {15} gives the time dependant coordinates of D and E. After simplification the closed-form expression for span length for the over-wrap case is given by

$$L(t) = \sqrt{d_0^2 + 2e\,d_0 \sin(\theta(t)) + e^2 - R_1^2 - 2R_1 R_2 - R_2^2}. \tag{16}$$

Dynamic equations for an eccentric roller

A sketch highlighting the forces acting on a web wrapped eccentric roller, the key distances, and the key angles that are required for writing the governing equations for the rotational motion of the eccentric roller is shown in Fig. 3.

Due to the rotation of the eccentric roller the web entry point on the surface of the roller varies, and as a result d_{en} and d_{ex} also vary. These must be taken into account in the angular position and angular velocity governing equations for the eccentric roller which are given by

$$\dot{\theta} = \omega$$
$$J\dot{\omega} = -b_f \omega - T_{i-1} d_{en} \cos\theta_{en} + T_i d_{ex} \cos\theta_{ex} + mge\sin\theta \tag{17}$$

where d_{en} is the distance between the entry point on the roller that is upstream of span $i-1$ and the center of rotation and d_{ex} is the distance between the exit point on the roller and the center of rotation. In {17}, d_{en}, d_{ex}, θ_{en}, θ_{ex} are all functions of θ and can be derived based on the analysis presented in the previous section.
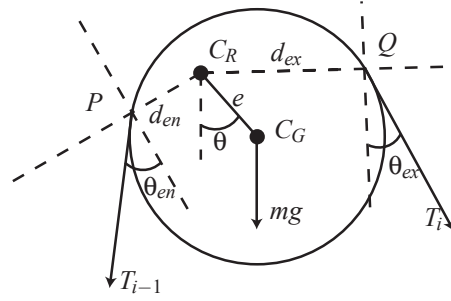
Figure 3: Eccentric idle roller: C_G is the geometric center, C_R is the center of rotation, e is the amount of eccentricity, P is the web entry point, Q is the web exit point, d_{en} is the distance between the center of rotation and the web entry point, and d_{ex} is the distance between the center of rotation and the web exit point.

Figure 4 shows the relationship between the angles at the entry contact point. Employing the cosine law, the following expression for the cosine of the angle θ_{en} can be obtained:

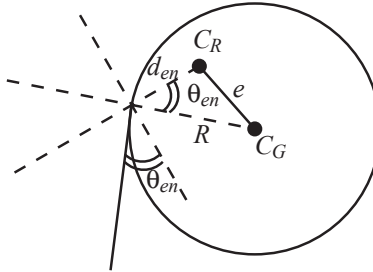$$\cos(\theta_{en}) = \frac{R^2 + d_{en}^2 - e^2}{2Rd_{en}}. \quad \{18\}$$

Figure 4: The angle θ_{en} is determined by using the the cosine law on the triangle with sides d_{en}, R and e.

To find d_{en}, it is required to find the coordinates of the points P and C_R in the same coordinate axes. Equation $\{6\}$ gives the coordinates of the point P in a coordinate axes having the origin at the geometric center of roller $i - 1$ and the x-axis aligned with line joining the geometric centers of the two rollers (note that in the case of eccentric roller the distance d between the geometric centers of the rollers is function of θ; therefore, P is also function of θ). The coordinates of the center of rotation C_R in this reference frame are (see fig. 5)

$$C_R = \begin{pmatrix} d_0 \cos(\alpha) \\ d_0 \sin(\alpha) \end{pmatrix}. \quad \{19\}$$

Using again the cosine law for angle α as in

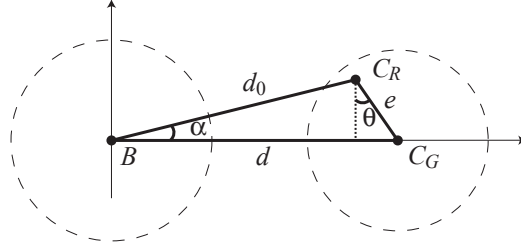$$e^2 = d_0^2 + d^2(\theta) - 2d_0 d(\theta) \cos(\alpha) \quad \{20\}$$

54

Figure 5: Figure to determine the coordinates of C_R in the frame having the x-axis aligned with the line joining the geometric centers of the rollers (for computation of d_{en} using {22}).

and replacing the expression of $d(t)$ in {9}, an expression for $\cos(\alpha)$ may be given by

$$\cos(\alpha) = \frac{d_0 + e\sin(\theta)}{d(\theta)}. \qquad \{21\}$$

Equipped with equations {6}, {19}, {21}, the expression for the distance $d_{en}(\theta)$ may be easily obtained:

$$d_{en}(\theta) = ||P(\theta) - C_R(\theta)||. \qquad \{22\}$$

A similar procedure may be used to determine d_{ex} and θ_{ex}.

From the analysis of the modified governing equations for web tension in a span and web velocity on an eccentric roller, it is possible to highlight the reasons for the presence of tension disturbances with higher order harmonics other than the rotation frequency of the roller. First, the appearance of the term $mge\sin\theta$ in the governing equation for the velocity on the eccentric roller indicates that there is a disturbance with frequency equal to the rotational frequency of the roller (the fundamental frequency of the tension disturbance). The governing equation for web tension {1} contains the angular velocity of the roller through two terms: $EAv_i = EAR_i\omega_i$ and $EA\dot{L} = EAd_0e\omega_i\cos\theta_i/L$. Because the angular velocity (ω_i) in the first term has the fundamental frequency of the disturbance, web tension will contain this frequency component also. Due to the multiplication of ω_i and $\cos\theta_i$ in the second term, the second order harmonic will be present in the tension signal. Since the web tension appears linearly in the governing equation of web velocity on the roller, it will induce oscillation in the velocity signal with the first and second harmonic. Because the surface velocity of the roller has the first and the second harmonic, the multiplication of ω_i and $\cos\theta_i$ will generate also the third harmonic, and so on. It is evident that the coupling between roller surface velocity and web tension creates the higher order harmonics in both web tension and web velocity. Understanding this coupling and the consequences of having eccentric rollers is critical in designing control systems to regulate web tension.

EXPERIMENTS AND MODEL SIMULATIONS

To validate the proposed model for eccentric rollers, the Euclid Web Line (EWL) is used as an experimental platform; a sketch of the platform configuration is shown in
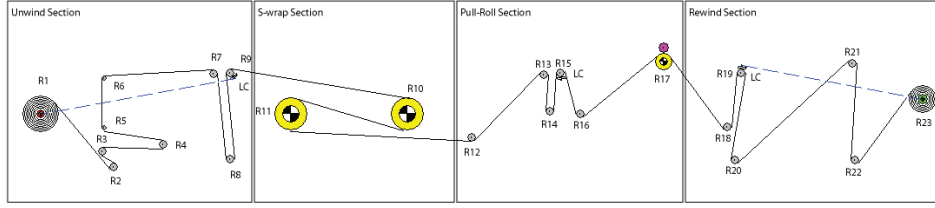
55

Figure 6: The Euclid Web Line (EWL).

Fig. 6. The EWL is composed of four sections: the unwind, the S-wrap, the pull roll, and the rewind sections. The unwind and rewind sections are under an outer-loop tension control with an inner-loop speed control, while the other two sections are under pure speed control. The S-wrap lead roller is eccentric. The idea is to use the models in [4] plus the model for eccentric rollers presented in this paper to simulate the entire EWL, and then compare the simulation data with the data collected from experimentation on the EWL. It is common practice to perform model validation in an open-loop setup, but this is not possible because the line cannot be run without feedback control. Therefore, the simulations of the web line will include a model of the various controllers together with the model of the web line. Also, we will focus on the unwind section because the eccentric S-wrap roller affects tension in the unwind section.

The goal of the simulation and experimental study is to determine whether the models will be able to reproduce steady-state oscillations that are found in the measured tension signal. For this reason it was chosen to conduct experiments at constant web speeds and analyze the frequency content of the tension signal using the Fast Fourier Transform (FFT) of the signal data obtained from both the experiments and model simulations.

At a given web velocity v, the fundamental frequency of the tension disturbance induced by the eccentric S-wrap roller is given by

$$f_0 = \frac{v}{10\pi R_S}. \qquad \{23\}$$

It is expected that the tension signal from both the model simulations and experiments will contain oscillations at the fundamental frequency and its harmonics at $2f_0, 3f_0, \ldots,$ etc. Moreover if the torque loss due to bearing friction is reasonably well known, it is expected that the amplitude of the tension oscillations from model simulations to match those from experiments. Experiments conducted in the unwind section of the EWL to determine friction loss due to idle rollers is discussed first followed by the results of experiments and model simulations to verify the models discussed in the paper.

Estimation of idle roller bearing friction

Due to the absence of speed feedback signals on the idle rollers, estimation of the idle roller friction parameter is a difficult task. A procedure that was used to estimate torque loss due to bearing friction in the idle rollers is given in the following; this torque loss estimate was used in the model simulation. The idea is to use measurements from

two pairs of load cells, each pair mounted on idle rollers which are separated by a known number of idle rollers in the unwind section of the EWL, i.e., there are a fixed number of idle rollers between two load cell rollers within the unwind section. To illustrate the procedure consider a simple configuration like the one shown in Fig. 7 with load cells on two consecutive identical idle rollers.
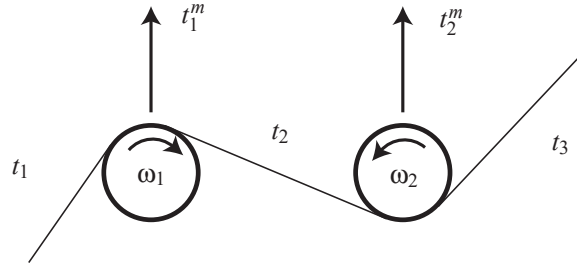

Figure 7: Simple Configuration for Identification of Bearing Friction Loss in Idle Rollers

The dynamic equations for the two rollers are

$$J\dot{\omega}_1 = -\tau_f + R(t_1 - t_2),$$
$$J\dot{\omega}_2 = -\tau_f + R(t_2 - t_3) \qquad \{24\}$$

where τ_f denotes the bearing friction torque. The tension measured by the load cells is an average of the tensions in adjacent spans, that is,

$$t_1^m = \frac{t_2 + t_1}{2}, \qquad t_2^m = \frac{t_3 + t_2}{2} \qquad \{25\}$$

where t_i^m denotes the tension measured by load cells on the ith roller. At the steady-state condition one can assume constant rotational speed for the idle rollers; from equations $\{24\}$ one can obtain the following:

$$0 = -\tau_f + R(t_1 - t_2)$$
$$0 = -\tau_f + R(t_2 - t_3) \qquad \{26\}$$

which gives

$$0 = -2\tau_f + R(t_1 - t_3). \qquad \{27\}$$

Since

$$t_1^m - t_2^m = \frac{t_1 - t_3}{2}, \qquad \{28\}$$

an expression for the friction torque is

$$\tau_f = R(t_1^m - t_2^m) \qquad \{29\}$$

This expression for the friction torque based on the two measurements only applies for this simple configuration. The EWL is equipped with two load cells in the unwind section, one at R3 and one at R9 (see Fig.6) and there are five additional idle rollers

including the two guide rollers. Following the same procedure as was done for the simple configuration, the equations at steady-state are

$$0 = -\tau_{f1} + R(t_1 - t_2)$$
$$0 = -\tau_{f2} + R(t_2 - t_3)$$
$$\vdots$$
$$0 = -\tau_{f7} + R(t_7 - t_8)$$

$\{30\}$

Addition of the above equations results in

$$\sum_{i=1}^{7} \tau_{fi} = R(t_1 - t_8).$$

$\{31\}$

By assuming

$$t_1^m \simeq t_1 \qquad t_2^m \simeq t_8,$$

$\{32\}$

it is possible to define the average friction torque as

$$\overline{\tau}_f = \frac{\sum_{i=1}^{7} \tau_{fi}}{7} = \frac{R(t_1^m - t_2^m)}{7}.$$

$\{33\}$

Note that the friction torque will depend on the angular velocity of the idle roller. The following friction model which is a linear combination of a constant term and a viscous term is considered:

$$\tau_f = -c - b\omega$$

$\{34\}$

To estimate the parameters, b and c, in $\{34\}$ the machine is run at N different line speeds. For each experiment the angular velocity of the idle rollers ω_i and the friction torque τ_{fi} are computed using $\{33\}$. This gives N pairs of (ω_i, τ_{fi}) that can be used to estimate the friction parameters b and c by solving the following minimization problem:

$$\min_{b,c} \sum_{i=1}^{N} (-c - b\omega_i - \tau_{fi})^2$$

$\{35\}$

For the friction model considered in $\{34\}$, this minimization problem is a linear regression.

Table 2 shows the results from a set of experiments performed on the EWL following the procedure described previously. The linear regression of the data reported in Table 2

Line speed [FPM]	100	150	200	250	300	350
ω [rad/s]	13.33	20	26.66	33.33	40	46.66
$t_1^m - t_2^m$ [lbf]	0.755	0.84	0.905	0.865	0.935	0.97

Table 2: Idle Roller Friction Loss Data at Various Line Speeds

gives the following values for the friction model coefficients:

$$c = 0.0127 \text{ [lbf ft]}, \qquad b = 1.054\text{e-}4 \left[\frac{\text{lbf ft}}{\text{rad/s}}\right]$$

$\{36\}$

58

Results

Figures 8(a) and 8(b) show the FFT of the tension signals from experiments and model simulations, respectively, for the line speed of 200 FPM. At this line speed the fundamental frequency of the tension oscillations due to eccentricity in one of the S-wrap rollers is $f_0 = 1.06$ Hz. The presence of the fundamental frequency of the S-wrap and its higher-order harmonics is evident from the experimental data. The same frequencies can be easily recognized in the FFT of the tension data from model simulations, and the amplitude of these tension oscillations are also comparable. Note that the FFT of the experimental data has disturbances at other frequencies because of the presence of other non-ideal rotating elements in the web line which are not included in the model simulation. Figure 9 and Figure 10 show results for line speeds of 250 FPM and 300 FPM.

CONCLUSIONS AND FUTURE WORK

In this paper a model for an eccentric roller was presented together with the derivation of an expression to compute the length of spans adjacent to the eccentric roller. The tension oscillations are caused by the coupling between the angular velocity of the eccentric roller and web tension in the spans adjacent to it. The model was validated by comparing the FFT of the tension data collected from an experimental platform and the tension data obtained from computer simulations of the presented model. The comparison showed good matching between experimental and model simulation data for various speed.

The results presented in this paper not only have value from the modeling point of view but also from the tension control stand point. In fact, by identifying the source and the type of the tension oscillations, one can effectively design tension control systems and improve performance. For example, since the tension oscillations are due to an internal nonlinearity (that is, eccentricity of the roller), it is not possible to reject such oscillations by using an internal model of the disturbance. Exploiting the improved knowledge on the model of the web line to develop tension controllers that reduce these tension oscillation is part of the future work. Another aspect that is not considered in the paper is web slip on the roller; this may be particularly relevant since the potential for web slip on an eccentric roller is high. Future work will also investigate web slip on an eccentric roller.

ACKNOWLEDGEMENTS

REFERENCES

1. Branderburg, G., "New mathematical model for web tension and register error," in Proceedings of the 3rd International IFAC Conference Instrumentation Automation Paper, Rubber Plastic Industry, 1977, pp. 411–438.

2. Shelton, J. J., "Dynamic of web tension control with velocity or torque," in Proceedings of the American Control Conference, 1986, pp. 1423–1427.

3.   Pagilla, P. R., Siraskar, N. B., and Dwivedula, R. V., "Decentralized control of web processing lines," IEEE Transactions on Control Systems Technology, vol. 15, January 2007, pp. 106–116.

4.   Branca, C., Pagilla, P. R., and Reid, K. N., "Modeling and identification of the source of oscillations in web tension," Proceedings of the Tenth Intl. Web Handling Conference, 2009.

5.   Branca, C., Pagilla, P. R., and Reid, K. N., "Computation of span length variations due to non-ideal rolls," Proceedings of the Tenth Intl. Web Handling Conference, 2009.
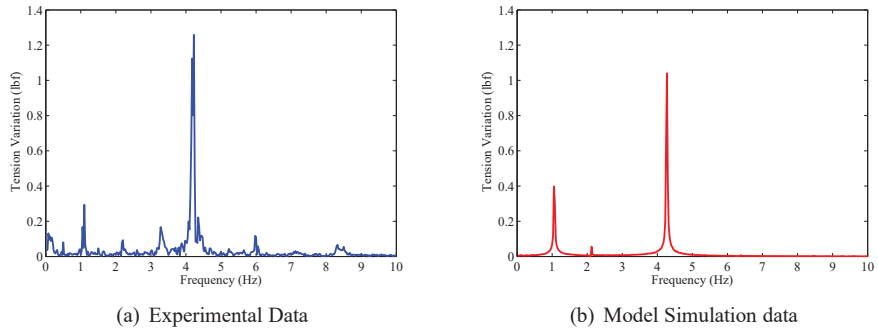
(a) Experimental Data   (b) Model Simulation data

Figure 8: Comparison of the FFT of tension signals with line speed 200 FPM.

(a) Experimental Data   (b) Model Simulated Data
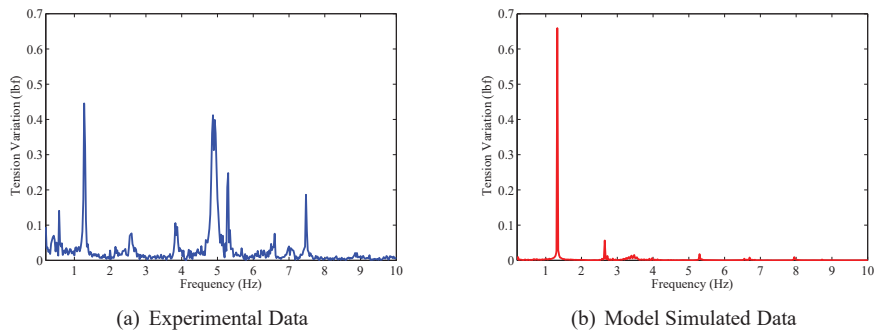
Figure 9: Comparison of the FFT of tension signals with line speed 250 FPM.

(a) Experimental Data   (b) Model Simulation Data
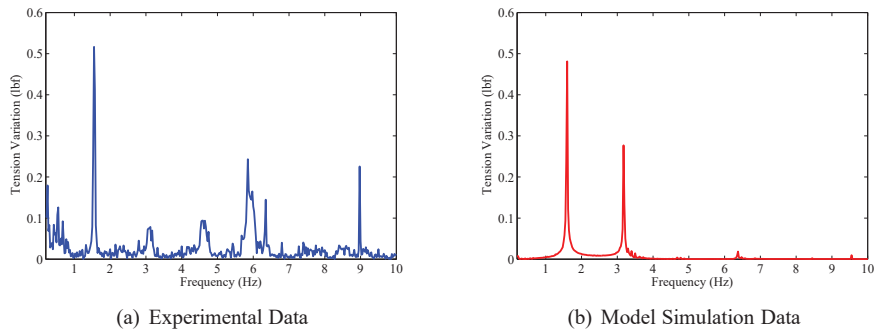
Figure 10: Comparison of the FFT of tension signals with line speed 300 FPM.

Name & Affiliation	Question
Jim Dobbs, 3M Company	Can you explain how you took into account the wrap angle changes on your rollers? You appear to be focusing only on change of the span length.
Name & Affiliation	**Answer**
Carlo Branca, Oklahoma State University	That comes directly from the span length changes.
Name & Affiliation	**Question**
Jim Dobbs, 3M Company	You are wrapping and unwrapping the eccentric roller and the neighboring rollers. Have you accounted for all the wrap angle changes for the web on those rollers?
Name & Affiliation	**Answer**
Carlo Branca, Oklahoma State University	It should be accounted for because the unwrapping of the roller is now part of the web span length.
Name & Affiliation	**Response**
Jim Dobbs, 3M Company	Maybe this is a small effect.
Name & Affiliation	**Question**
Marko Jorkama, Metso Paper	Where do you get the value for the eccentricity in your model?
Name & Affiliation	**Answer**
Carlo Branca, Oklahoma State University	We estimate it by observing the roller. You can see it as it spins.
Name & Affiliation	**Question**
Marko Jorkama, Metso Paper	I would think that the eccentricity depends on speed. You call it eccentricity, but I think it is vibration.
Name & Affiliation	**Answer**
Carlo Branca, Oklahoma State University	You can observe the roller is not perfect.
Name & Affiliation	**Response**
Marko Jorkama, Metso Paper	When you increase the speed, the vibration will increase and what you call eccentricity will also increase like roller whirl.
Name & Affiliation	**Question**
Tim Walker, TJWalker & Associates	In your experimental data I don't see a baseline tension. You just show variation.
Name & Affiliation	**Answer**
Carlo Branca, Oklahoma State University	It is around 20 pounds or 89 Newtons.
Name & Affiliation	**Question**
Frank Hoffman, Windmoeller & Hoelscher	In your figure with the experimental and simulated data one can see impressive, good results at 200 fpm. The results change with speed. The model does not produce as good results at 250 and 300 fpm. Can you explain?
Name & Affiliation	**Answer**
Carlo Branca, Oklahoma State University	The model is really very sensitive to friction parameters. This procedure does not give you an exact result, just an

estimation. It does work better for some velocities than others. The results depend on having a good friction model for all rollers. We don't have a direct method to obtain a very good model. This model yields an estimate and it works well.

Name & Affiliation	Question
Doug Offerhaus , Catalyst Paper	How does your model apply to rolls of paper that are round and concentric on one end but out-of-round and eccentric on the other end? This is a common condition.

Name & Affiliation	Answer
Carlo Branca, Oklahoma State University	This is part of my dissertation and I haven't finished the work yet. I am looking into it.

Name & Affiliation	Question
Gunther Oedl, Brueckner	In your governing equation there are two influences. One is eccentricity, a purely geometric number, and the other is the unbalance of a roller. Could you separate those influences which are completely different? It is not necessary that the center of gravity and the geometric center of the roller are coincident.

Name & Affiliation	Answer
Carlo Branca, Oklahoma State University	There would be no change of span length for the unbalanced roller.

Name & Affiliation	Question
Gunther Oedl, Brueckner Machinery	Does your model predict what happens if the roller is unbalanced when the roller has zero eccentricity?

Name & Affiliation	Answer
Carlo Branca, Oklahoma State University	We have focused only on eccentricity. I assume the center of geometry and the center of gravity are coincident. We can add unbalance.